



Electrodeposition of lead dioxide on carbon substrates from a high internal phase emulsion (HIPE)

P.J. BLOOD¹, I.J. BROWN¹ and S. SOTIROPOULOS^{2,*}

¹School of Chemical, Environmental and Mining Engineering, The University of Nottingham, University Park, Nottingham NG7 2RD, UK

²Department of Chemistry, Aristotle University of Thessaloniki, Thessaloniki 54124, Greece

(*author for correspondence, fax: +30 2310 443922, e-mail: eczss@chem.auth.gr, eczss@otenet.gr)

Received 11 March 2003; accepted in revised form 29 July 2003

Key words: electrodeposition, emulsions, PbO₂ electrodes, porous media

Abstract

PbO₂ coatings on carbon electrode substrates were produced by anodic electrodeposition from a stationary high internal phase emulsion (HIPE) with the bath components added in the water phase. The deposits have a distinct structure consisting of 10–50 μm high pyramidal aggregates, pitted with smaller pores. This is attributed to the growth of the deposits through the aqueous network of the HIPE emulsion that is, through the tortuous paths formed by its interconnected water cavities. The coatings thus produced are characterised by enhanced electrochemical activity towards the PbO₂/PbSO₄ transformation.

1. Introduction

The electrodeposition of Pb and PbO₂ on lightweight carbon or reticulated vitreous carbon (RVC) supports has been suggested for the production of alternative composite electrodes in lead-acid batteries [1, 2]. Lead acid battery cells based on carbon supported active material have been tested in an attempt to decrease the dead battery weight and increase the active mass utilisation through the thin layers used [3]. At the same time, industrial PbO₂ anodes are used in a number of electrosynthetic processes such as the regeneration/production of chromates, perchlorate and ozone production [4] as well as the oxidative destruction of pollutants (e.g. cyanide ions [5, 6]). They too, are frequently formed by anodic electrodeposition on carbon, Ti and Ebonex[®] substrates [7–9].

Electroplating from immiscible water-organic solvent systems using two-layer baths has been employed for the production of metal powders [10] whereas that from dispersions is used for the production of composite materials [11]. Plating from mixed but macroscopically homogeneous systems has recently appeared in the electrochemical literature mainly due to the work of Attard, Bartlett and co-workers who produced nanoporous deposits using concentrated surfactant solutions as liquid crystalline templates (see for example references [12, 13]) and to Brown et al. [14] who electroplated macroporous Ni from a high internal phase emulsion (HIPE). HIPEs are emulsions with a very high content of the dispersed phase (in excess of 75% v/v). The latter

is organised in deformed polyhedral droplets dispersed in the continuous phase and having relatively large contact areas resulting in a network of interconnected cavities [15, 16]. Upon polymerisation of the oil phase of water-in-oil HIPEs a generic type of polymers (PHIPEs) is formed, having a characteristic porous cell structure indicative of that of the precursor HIPE [16]. We have already presented the use of water-in-oil HIPE emulsions and PHIPE polymers as liquid and solid porous media for Ni electrodeposition [14, 17–19].

The aim of this work is to investigate the formation and characterisation of PbO₂ electrodeposits on graphite substrates, grown anodically from HIPE emulsions. Its objectives are

(i) demonstration of the feasibility of the technique, not only for cathodic [14], but also for anodic electrodeposition processes, (ii) microscopic characterisation of the PbO₂ deposit morphology and its interpretation based on electrodeposition conditions through the HIPE medium and (iii) electrochemical characterisation of the deposits by means of the PbO₂ to PbSO₄ transformation and comparison with smooth deposits on graphite and on RVC.

2. Experimental

2.1. HIPE emulsion preparation

The emulsions prepared in this work were 80% v/v dispersed aqueous phase in continuous oil phase. These

were produced by adding 400 cm³ of the aqueous phase in 100 cm³ of the oil phase under continuous mixing in an appropriate stainless steel vessel equipped with a mixer (details of the preparation procedure and setup have been presented elsewhere [14, 17–19]). The aqueous phase was the PbO₂ deposition bath made up with doubly distilled water (the exact bath composition is given in 2.2 below). The oil phase in standard experiments had the same v/v composition as that of references [14, 17–19]: 15% styrene (Aldrich, 99%), 62% 2-ethyl-hexyl-acrylate (Aldrich, 98%), 8% divinylbenzene (Aldrich, 99+% ACS) and 15% sorbitan monooleate (Aldrich, 99+% ACS). In a few control experiments 2-ethyl-hexyl-acrylate was replaced by styrene (a variation known to change only the mechanical properties of the resulting polymer but have no change to either the polymer or precursor emulsion structure [20]); in another set of control experiments the surfactant sorbitan monooleate content was increased from 15 to 30% with a corresponding decrease of 2-ethyl-hexyl-acrylate from 62 to 47% (an increase in surfactant concentration is known to result in smaller but more open cells i.e. having a large number of pores [16]). The modified HIPE emulsions containing the components of the deposition bath were stable for at least 8 h at the deposition temperature of 60 °C when no polymerisation initiator was present. For the production of the corresponding PHIPE polymers by emulsion polymerisation, 1% w/w potassium persulphate (Aldrich, 99% +), acting as the initiator, was added in the water phase and polymerisation was carried out at 60 °C for 6 h in sealed vials.

2.2. PbO₂ electrodeposition

Lead dioxide electrodeposition was carried out from a lead nitrate-copper nitrate bath [7] (325 g l⁻¹ Pb(II) nitrate, Aldrich 99+% ACS; 50 g l⁻¹ Cu(II) nitrate hemipentahydrate Aldrich 98% ACS; total ionic strength of 3.6 M) at 60 °C by immersion of the electrochemical cell in a thermostated water bath. The function of copper ions is to deposit on the cathode as metallic copper hence to minimise Pb(II) ion deposition on the cathode which would decrease the efficiency of their oxidation to Pb(IV) and deposition as PbO₂ on the anode. In a few control experiments the ionic strength of the deposition bath used as the internal phase of the emulsion was adjusted to the higher value of 6.4 M with addition of appropriate quantity of KNO₃.

The cell was a simple cylindrical vial of a 3 cm diameter and a 6 cm height. A carbon graphite rod (3 mm diameter, 99.997%, Goodfellow Ltd.) was used as the anode (electrodeposition substrate) with a 5 mm length exposed to the plating solution, thus resulting in a total exposed geometric area of 0.542 cm² (including tip area). The unexposed portion of the carbon rod was encased within a glass rod and sealed at the end using PTFE tape. In some experiments the anode was a 0.5 cm × 0.5 cm × 1 cm RVC parallelepiped of a 6 cm²

true surface area (The Electrosynthesis Co Inc., 30 ppi, 24 cm⁻¹ specific surface area [21]). A cylindrical stainless steel mesh attached to the cell inner wall (AISI 304, 26 × 26 wires per inch, 0.25 mm thick, Goodfellow Ltd.) was used as the cell cathode. Electrical contacts between the anode and cathode electrodes and the copper wire current collectors were made with conductive carbon cement (WPI Inc.) The interelectrode gap was 8.25 mm and electrodeposition was carried out at a current density of 3.2 mA cm⁻² (per real surface area) in all cases using the galvanostatic mode of operation of an EG&G Princeton Applied Research 263A electrochemical station. Before electrodeposition the carbon substrates were pretreated by immersion in 10% (v/v) nitric acid (70%, Fisher Chemicals) for 20 min followed by thorough washing with Millipore[®] water.

2.3. Characterisation of PbO₂-coated electrodes

The electrochemical characterisation of all PbO₂-coated carbon samples with respect to its electrochemical transformation to PbSO₄ was carried out by means of cyclic voltammetry at a 10 mV s⁻¹ potential sweep rate in deaerated 0.5 M H₂SO₄ solutions (double distilled sulphuric acid, PPB/Teflon[®] grade, Aldrich) at 20 °C. A three-electrode cell with a Pt coil counter electrode (BAS Technicol Ltd) and a Saturated Calomel Electrode (SCE, EG&G) equipped with a salt bridge ending to a Vycor[®] tip (EG&G), were used in these experiments which were performed with the help of an EG&G Princeton Applied Research 263A Potentiostat controlled *via* a 486 personal computer running the EG&G Research Electrochemistry Software v.4.30.

For the microscopic characterisation of the deposits by Scanning Electron Microscopy (SEM) a Hitachi S-570 SEM was used, while a Siemens Kristalloflex Diffractometer XRD unit running Diffrac-AT analytical software was employed for X-ray diffraction characterisation of the PbO₂ deposits.

3. Results and discussion

3.1. Structure of PHIPE produced from HIPE emulsions

The SEM micrograph of Figure 1 shows the structure of the PHIPE polymer produced by emulsion polymerisation from the modified HIPE emulsion containing the components of the lead dioxide electrodeposition bath in the dispersed aqueous phase. The polymer is made up of cells having a 10 μm average diameter and corresponding to the water droplets of the precursor emulsion. These cells are interconnected *via* small pores, typically 1–5 μm in diameter, corresponding to the contact areas between the water droplets of the emulsion. There is very little, if any, change in this polymer structure when compared to that of the polymer made from an emulsion with a pure water phase, as presented in many SEM micrographs elsewhere [14, 17–19]. Since

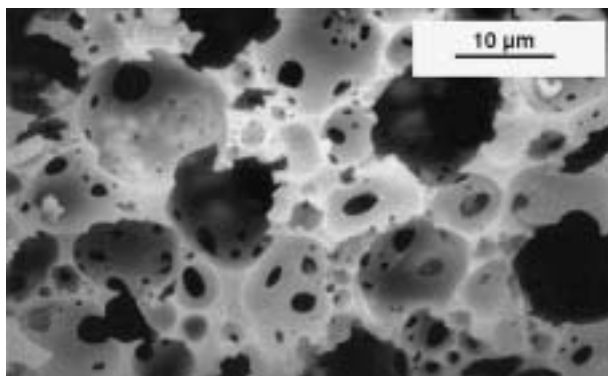


Fig. 1. SEM micrograph of PHIPE polymer produced from a modified HIPE emulsion containing the PbO_2 electrodeposition bath components (325 g l^{-1} lead nitrate + 50 g l^{-1} copper nitrate hemipentahydrate).

it is accepted that the PHIPE structure is indicative of the precursor HIPE organisation [15, 16], it follows that the presence of the lead dioxide plating salts (at the standard concentration levels given in 2.2 above, and corresponding to a total ionic strength of 3.6 M) in the aqueous phase has no significant effect on the structure of the HIPE emulsion. This is in contrast with the effect of the presence of a nickel sulphamate plating bath in the aqueous phase that we reported in Reference [14]. At the higher salt concentrations and ionic strength of that study (600 g l^{-1} nickel sulphamate + 10 g l^{-1} nickel chloride + 40 g l^{-1} boric acid, total ionic strength of 6.4 M) we found a ‘wall-thickening’ effect on the structure of PHIPE and HIPE, resulting in smaller cell sizes and a decrease in pore density (that effect was attributed to increased adsorption of the surfactant emulsifier at the oil-water interface and an increase in the volume of the oil phase microdomains, due to a significant ‘salting-out’ effect in the presence of the large quantities of nickel salts [16]). It should be noted that, when the ionic strength of the Pb containing aqueous phase of the emulsion was adjusted to 6.4 M (with the addition of KNO_3), a similar small and closed cell structure was obtained. The more open structure of the HIPE containing the standard PbO_2 bath of a 3.6 M ionic strength (Figure 1) from that containing the standard Ni bath of 6.4 M (Figure 1(B), [14]) may be one of the reasons for the different types of deposits formed in each case, as discussed below.

3.2. Production of porous PbO_2 coatings by electrodeposition from HIPE emulsions

Figure 2(A) and (B) present the SEM micrograph of a PbO_2 coating deposited on a carbon electrode for 21 600 s at a current density of 3.2 mA cm^{-2} , from a HIPE emulsion containing the components of the standard bath (a similar picture was obtained when the acrylate monomer was replaced by styrene, with no effect to emulsion structure [20]). The deposit has a ragged structure and is composed of pyramidal features

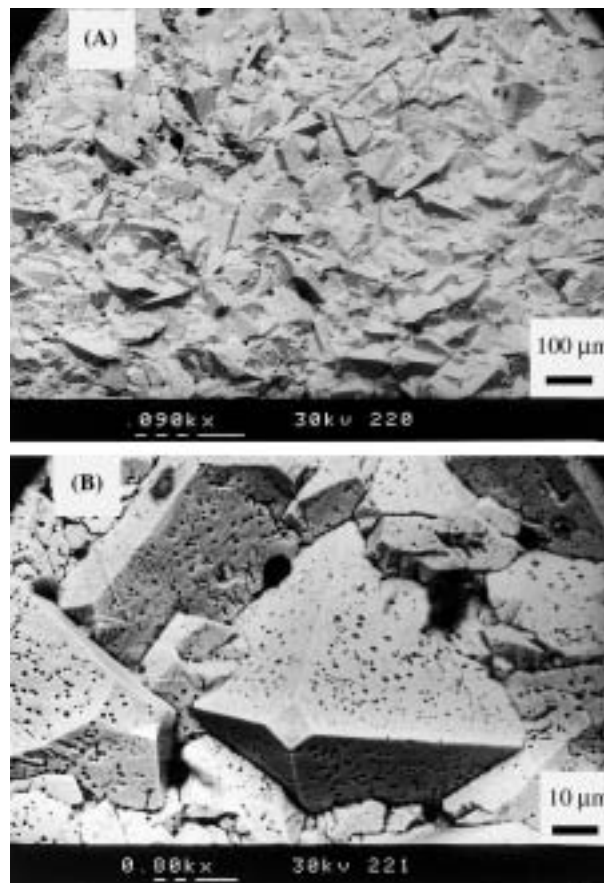


Fig. 2. SEM micrographs of a PbO_2 electrodeposit produced at 3.2 mA cm^{-2} for 21 600 s from a HIPE emulsion on a carbon rod electrode substrate, at two different magnifications (A) and (B), as indicated by the bar dimensions shown in the micrographs.

10–50 μm in height i.e. of dimensions similar (slightly larger) to those of the PHIPE cells of Figure 1. The substrate surface coverage was typically more than 85% (as determined by image analysis of the entire sample area) and the faradaic efficiency (as determined by calculation of the deposition charge and gravimetric analysis) was typically 90%. Furthermore, as can be seen in the details of Figure 2(B) the lead dioxide pyramidal structures are pitted with a high number of pores having diameters ranging from 0.5 to 2 μm , suggesting that the deposit possesses surface porosity. Figure 3(A) and (B) present the SEM micrographs of a similar PbO_2 coating deposited on a carbon electrode for a shorter period of 14 400 s at the same current density of 3.2 mA cm^{-2} , from a HIPE emulsion. These show the first stages of deposit formation and reveal that the polyhedrals that this is made of have a reticulated structure.

Figure 4(A) and (B) present SEM micrographs of PbO_2 deposits produced at the same current density of 3.2 mA cm^{-2} on a carbon rod and a 30 ppi RVC substrate, respectively, from plain aqueous baths. The surface coverage was close to 100% in both cases and the faradaic efficiency in excess of 99 and 95% respectively. None of the features of the deposits prepared from the HIPE baths could be observed but instead, a

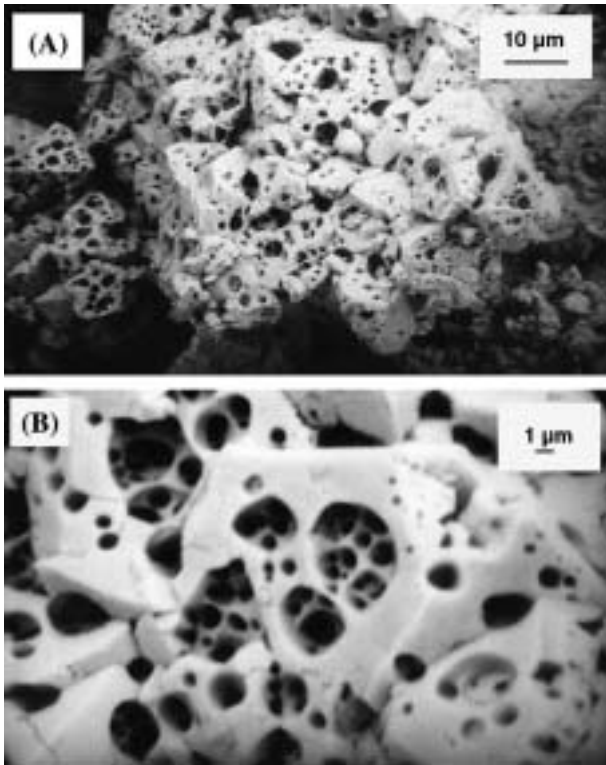


Fig. 3. SEM micrographs of a PbO_2 electrodeposit produced at 3.2 mA cm^{-2} for 14 400 s from a HIPE emulsion on a carbon rod electrode substrate, at two different magnifications (A) and (B), as indicated by the bar dimensions shown in the micrographs.

relatively even, nodular deposit was obtained. In control experiments, where the aqueous bath contained the surfactant sorbitan monooleate alone, at the 15% v/v levels of the emulsion formulation, a similar even deposit was obtained.

Finally, XRD analysis of deposits produced from plain lead/copper nitrate aqueous baths had a 74% β - PbO_2 –26% α - PbO_2 composition whereas those produced from modified HIPE had a similar 80% β - PbO_2 –20% α - PbO_2 composition. This is in accordance with the literature [2, 7] where it is reported that from unbuffered neutral or acidic baths β - PbO_2 is the predominant form (70–80%) of anodically grown lead dioxide.

The special structure of the HIPE-produced deposit may therefore be attributed to the distortion of the electric field caused by the presence of the non-conducting oil phase shell structure within the HIPE emulsion. Provided that the deposit growth does not affect the emulsion structure drastically, electrodeposition within an aqueous cell starts from the openings/pores closer to the electrode substrate surface and the deposit grows within each cell in directions corresponding to minimum ohmic losses and mass transfer limitations i.e. preferably along paths linking the entrance pore with the other pores of the cell, a situation which could explain the reticulated structure of the deposit during the initial stages of its development as depicted in Figure 3(A) and (B). This would finally result in the formation of pyramidal structures within each aqueous cell, with

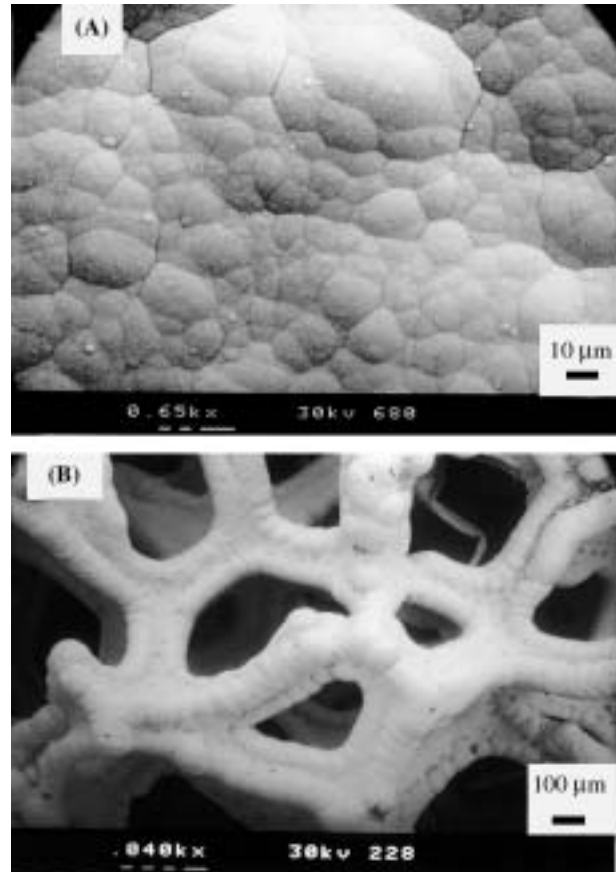


Fig. 4. SEM micrographs of PbO_2 electrodeposits produced at 3.2 mA cm^{-2} from a plain aqueous bath at (A) a carbon rod electrode substrate and (B) a 30 ppi RVC electrode substrate.

each pyramid point corresponding to a contact point-pore between two adjacent cells, similar to the situation depicted in Figure 2(A) and (B). The microporosity of the pyramidal aggregates may be due to incomplete filling of the reticulated structure of Figure 3(A) and (B), as well as to slightly increased local current densities at the growing front of the ragged deposit and to partial lead ion depletion within each water cell. Elevated local current densities and mass transfer limitations are known to increase deposit irregularity whereas the former may also lead to a certain extent to faradaic efficiency losses associated with oxygen evolution and result in pitting.

There is a notable difference between the relatively uniform and reproducible pattern of the PbO_2 electrodeposits formed through HIPE and the irregular, highly pitted and uneven Ni electrodeposits produced under similar conditions [14]. We believe that this difference is due to a drastic change of the emulsion structure as the Ni deposit grows in the latter case whereas limited changes occur during the growth of PbO_2 . This hypothesis is further supported by the fact that prolonged electroplating of Ni resulted in macroscopically observed phase separation of the HIPE emulsion but no such effect was observed after prolonged PbO_2 deposition. Rearrangement of the emulsion during Ni plating may be explained by the more closed structure of the emulsion

containing the Ni plating bath of a high ionic strength of 6.4 M (see Figure 1(B) in [14]) as well as the low overpotential for hydrogen evolution at Ni. The closed structure results in a conductivity decrease and thus accentuation of current distribution inhomogeneities which in turn lead to high local current densities and a decrease in current efficiency (typically 70–80% at 5 mA cm^{-2}); the hydrogen gas evolved could lead to local emulsion phase separation. Interestingly enough, when the ionic strength of Pb containing HIPE was adjusted to the same level (6.4 M), no adherent lead dioxide deposit could be obtained. In contrast, the open structure of the HIPE emulsion in the presence of PbO_2 bath of a lower ionic strength of 3.6 M (see Figure 1) ensures a higher conductivity through the network of interconnected water domains, hence a more even current distribution. Thus, moderate local current densities are encountered and this, together with the low oxygen evolution overpotential at PbO_2 , results in higher current efficiencies (typically 90% at 3.2 mA cm^{-2}) and limited oxygen evolution. Thus the PbO_2 deposit slowly grows through the water domains of the precursor HIPE emulsion without extensively affecting its structure.

3.3. Electrochemical characterisation of PbO_2 coatings by means of cyclic voltammetry in sulphuric acid

The PbO_2 -coated electrodes of 3.2 were tested in 0.5 M H_2SO_4 deaerated solutions by means of cyclic voltam-

metry at a scan rate of 10 mV s^{-1} , in the $\text{PbO}_2/\text{PbSO}_4$ couple potential region of 0–2.00 V vs. SCE. The potential sweeps were initiated at the cell rest potential and scanned towards negative potentials i.e. towards the $\text{PbO}_2 + 3\text{H}^+ + \text{HSO}_4^- + 2\text{e}^- \rightarrow \text{PbSO}_4 + 2\text{H}_2\text{O}$ electrochemical surface reaction (the positive plate discharge reaction in a lead acid battery). Figure 5(A) presents the stabilised response (12th scan in this case) of the porous lead dioxide deposit produced from HIPE and shown in the SEM micrographs of Figure 2(A) and (B). Both the $\text{PbO}_2/\text{PbSO}_4$ and $\text{PbSO}_4/\text{PbO}_2$ transformations are depicted as well-defined peaks at +1.20 and +1.65 V vs. SCE respectively. The shape and potential range of these peaks are in agreement with those found in the literature for the lead dioxide/lead sulphate electroactive couple [2, 22]. The few scans needed to attain a stable voltammetric picture are most likely due to the electrochemical activation of the electrocatalyst as it enters the oxygen evolution region where organic impurities, particularly present in deposits produced from emulsions, are oxidised or physically removed. Figure 5(B) presents the stabilised cyclic voltammogram of the non-porous lead dioxide coating produced from an aqueous bath under the same electrodeposition conditions (3.2 mA cm^{-2} , 21 600 s, 60 °C) and shown in Figure 4(A). Finally, Figure 5(C) shows the stabilised voltammogram of the PbO_2 -coated RVC substrate of Figure 4(B).

The charge associated with the reduction of lead dioxide to lead sulphate was calculated for each

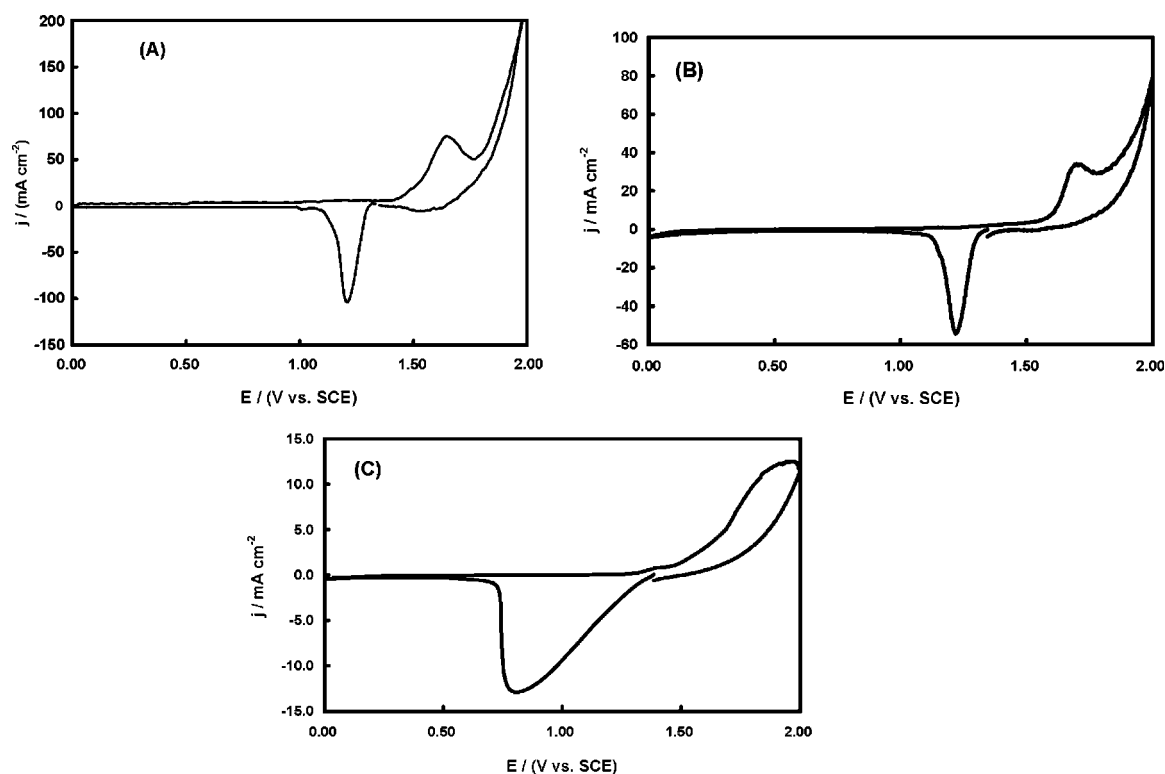


Fig. 5. (A) Voltammogram recorded at a potential scan rate of 10 mV s^{-1} in a deaerated 0.5 M H_2SO_4 solution, at a PbO_2 -coated carbon rod electrode produced by electrodeposition at 3.2 mA cm^{-2} from a HIPE emulsion; (B) Same as before but for a PbO_2 -coated carbon rod electrode produced by electroplating at 3.2 mA cm^{-2} from a plain aqueous bath; (C) Same as before but for a PbO_2 -coated 30 ppi RVC electrode produced by electrodeposition at 3.2 mA cm^{-2} from a plain aqueous bath.

Table 1. Porosity, thickness and mass specific reduction charge of lead dioxide deposits tested

Type of lead dioxide deposit	Deposit porosity ^a /%	Deposit thickness ^b / μm	PbO ₂ reduction charge per unit mass of material ^c /mC g ⁻¹
Electrodeposit from modified HIPE on graphite (3.2 mA cm ⁻² , 21 600 s, 60 °C)	40	150	11 053
Electrodeposit from plain aqueous bath on graphite (3.2 mA cm ⁻² , 21 600 s, 60 °C)	<6	84.5	3039
Electrodeposit from plain aqueous bath on 30 ppi RVC (3.2 mA cm ⁻² , 21 600 s, 60 °C)		50–75	12 246

^a The porosity of the coatings was calculated from the volume (calculated from the thickness) and mass of the PbO₂ coating (measured by weighing the substrates before and after electroplating).

^b The thickness of the coatings was measured using a micrometer and SEM micrographs.

^c Calculated by integration of the cathodic peak of the sample cyclic voltammogram at 10 mV s⁻¹ in 0.5 M H₂SO₄.

voltammogram from the area under the corresponding cathodic peak. For specimens of different geometric characteristics and dimensions it is more appropriate to report this charge per unit mass of deposit. This is also more relevant to situations where weight is an important parameter e.g. for battery materials. The charge per gram of lead dioxide coating was determined using the deposit mass as found gravimetrically after the electro-deposition process. The results of this charge analysis for the typical samples of Figures 2 and 4 are summarised in Table 1 together with the coating thickness and porosity characteristics.

Before departing on a comparison of the lead dioxide coatings with respect to their electrocatalytic activity based on the above-mentioned lead dioxide reduction charge per unit mass, we should comment on the significance of this quantity. First, it is not representative of the true surface area of the material since it is not based on a physical property of the material such as gas physisorption (used in BET analysis) but on an electrochemical surface reaction which is also dependant on ohmic losses and the effect of microstructure and reaction product conductivity on it. Second, it is directly related to the electroactive surface area for the particular reaction of PbO₂ reduction to PbSO₄ and hence relevant to the assessment of the material as a positive lead-acid battery plate material (and not necessarily as an industrial anode). Even in this case though, it is only characteristic of the particular scan rate and currents encountered during the cyclic voltammetric experiments presented here (an accurate evaluation of them as battery materials would require their slow discharge at low current densities). However, the reduction charge calculated from voltammetric experiments can still be considered a simple and fast test for an indicative assessment of lead dioxide electroactive surface area.

From Table 1 it follows that deposits produced on a carbon rod substrate by electrodeposition from a HIPE emulsion show at least a threefold increase in electroactive surface area per mass of deposit from those produced by electrodeposition from plain aqueous solutions. Although this increase is significant, it is lower than one should expect for an increase in porosity

from 6 to 40%. This may be due to the fact that the growth of voluminous and poorly conducting PbSO₄ on the outer surface of the coating limits the utilisation of the inner porous material of the HIPE-produced deposits. From the same table, lead dioxide electrodeposits produced by electrodeposition from HIPE appear to have comparable electroactive surface areas per unit mass with those produced from plain solutions on RVC (an alternative for light-weight lead-acid battery plates [2, 3]). The RVC-based electrodes have the advantage of smaller weight whereas the HIPE deposits are characterised by a smaller electrode volume which could also minimise ohmic losses.

4. Conclusions

As an extension to a similar cathodic electrodeposition process [14] we present here the formation of anodic PbO₂ electrodeposits from appropriate water-in-oil emulsions. Carbon electrode substrates were coated with porous lead dioxide *via* anodic electrodeposition from a stationary HIPE containing the components of the electrodeposition bath in the aqueous phase. The resulting deposits are organised in 10–50 μm high pyramidal aggregates, pitted with smaller pores. Although there is no exact host–guest relationship between the water droplets in the emulsion and the deposit structure, the latter is expected to be determined by its growth through the aqueous interconnected domains of the emulsion and the conductivity and mass transfer restrictions imposed by the network of this porous medium. Its fine features can be attributed to high local current densities and Pb ion depletion in the tortuous path of the emulsion aqueous domains through which the deposit grows. Simple voltammetric experiments show that PbO₂ coatings produced from HIPE emulsions by electrodeposition at *c.a.* 3 mA cm⁻² onto flat graphite substrates exhibit enhanced electroactive surface areas per mass of coating for their transformation to PbSO₄, when compared to anodic deposits produced from plain aqueous solutions onto the same substrate, and have comparable performance with deposits produced on RVC substrates.

Acknowledgements

The authors wish to thank the University of Nottingham (UK) for a Research Opportunity Fund scholarship to P.J.B. and EPSRC (UK) for a studentship to I.J.B. S.S. acknowledges a Science for Peace (SfP 977986) NATO grant.

References

1. A. Czerwiński and M. Żelazowska, *J. Electroanal. Chem.* **410** (1996) 55.
2. A. Czerwiński and M. Żelazowska, *J. Power Sources* **64** (1997) 29.
3. K. Das and A. Mondal, *J. Power Sources* **89** (2000) 112.
4. D. Pletcher and F.C. Walsh, in *'Industrial Electrochemistry'*, (Blackie Academic and Professional, 2nd edn, 1993), Ch. 7, pp. 364–370, Ch. 5, pp. 282–286.
5. P. Tissot and M. Fragniere, *J. Appl. Electrochem.* **24** (1994) 513.
6. D.R. Gabe, *Trans IMF* **75** (6) (1997) B131.
7. K.C. Narasimham and V.K. Udupa, *J. Electrochem. Soc.* **123** (1976) 1294.
8. Ch. Comninellis and E. Plattner, *J. Appl. Electrochem.* **12** (1992) 399.
9. A.H. Ras and J.F. Van Staden, *J. Appl. Electrochem.* **29** (1999) 313.
10. A. Calusaru, in C. Laird (Ed.), *'Electrodeposition of Metal Powders, Materials Science Monographs'*, Vol. 3 (1979), Ch. XX, pp. 390–398.
11. A.K. Graham (Ed.), *'Electroplating Engineering Handbook'* (Van Nostrand, Princeton NJ, 1971).
12. G.S. Attard, P.N. Bartlett, N.R.B. Coleman, J.M. Elliott, J.R. Owen and J.H. Wang, *Science* **278** (1997) 838.
13. J.M. Elliott, G.S. Attard, P.N. Bartlett, N.R.B. Coleman, D.A.S. Merkel and J.R. Owen, *Chem. Mater.* **11** (1999) 3602.
14. I.J. Brown and S. Sotiropoulos, *Electrochimica Acta* **46** (2001) 2711.
15. K.J. Lissant (Ed.), *'Emulsions and Emulsion Technology'*, Part I, Ch. 1 (Marcel Dekker, NY, 1974).
16. N.R. Cameron and D.C. Sherrington, *Adv. Polymer Sci.* **126** (1996) 163.
17. I.J. Brown, D. Clift and S. Sotiropoulos, *Mater. Res. Bull.* **34**(7) (1999) 1055.
18. I.J. Brown and S. Sotiropoulos, *J. Appl. Electrochem.* **30** (2000) 107.
19. I.J. Brown and S. Sotiropoulos, *J. Appl. Electrochem.* **31** (2001) 1203.
20. I.J. Brown, PhD Thesis, University of Nottingham, (2001).
21. D. Pletcher, I. Whyte, F.C. Walsh and J.P. Millington, *J. Appl. Electrochem.* **21** (1991) 659.
22. A. Czerwiński, M. Żelazowska, M. Grdeń, K. Kuc, J.D. Milewski, A. Nowacki, G. Wójcik and M. Kopczyk, *J. Power Sources* **85** (2000) 49.